[UCI]I804:24011-200000265216

2016년 2월

석사학위 논문

SIRT1 activators promote neuronal differentiation in human bone marrow mesenchymal stem cells

조선대학교 대학원

생명과학과

조 이 슬

SIRT1 activators promote neuronal differentiation in human bone marrow mesenchymal stem cells

인간의 골수 유래 중간엽 줄기세포에서 SIRT1 활성제를 통한 신경분화 촉진

2016년 2월 25일

조선대학교 대학원

생명과학과

조 이 슬

SIRT1 activators promote neuronal differentiation in human bone marrow mesenchymal stem cells

지도교수 조 광 원

이 논문을 이학석사학위 신청 논문으로 제출함

2015년 10월

조선대학교 대학원

생명과학과

조 이 슬

조이슬의 석사학위논문을 인준함

위원장 조선대학교 부교수 조 태 오 (인)

위 원 조선대학교 부교수 이 준 식 (인)

위 원 조선대학교 부교수 조 광 원 (인)

2015년 11월

조선대학교 대학원

CONTENTS

LIST OF FIGURES

Part I

Part II

LIST OF TABLE

Part I

Part II

ABBREVIATIONS

AMPK	AMP-activated protein kinase
BHA	butylated hydroxyanisole
BM-MSCs	bone marrow-mesenchymal stem cells
cAMP	cyclic adenosine monophosphate
Ctrl-MSCs	Control-MSCs
dMSCs	differentiated MSCs
DMSO	dimethyl sulfoxide
EX-MSCs	EX527 treated-MSCs
FBS	fetal bovine serum
MTT	(4,5-dimethylthiazol-2-yl-) 2,5-diphenyltetrazolium bromide
PBS	phosphate-buffered saline
PCR	polymerase chain reaction
PDE	phosphodiesterase
qPCR	quantitative PCR (or real-time PCR)
Roli-MSCs	rolipram treated-MSCs
RSV-MSCs	resveratrol treated-MSCs
RT	room temperature
SD	standard deviation
SIRT1	sirtuin1.

ABSTRCT

SIRT1 activators promote neuronal differentiation in human bone marrow mesenchymal stem cells

I-Seul Joe
Advisor : Assistant Prof. Goang-Won Cho, Ph.D.
Department of life science,
Graduate school of Chosun University

Human mesenchymal stem cells (hMSCs), which have the capacity to differentiate into neurons, have been used in regenerative medical therapies for neurodegenerative disorders. However, the differentiation potency of donor stem cells should be improved prior to engraft, which limits their therapeutic efficacy. Many researchers have shown that activation of sirtuin1 (SIRT1) have functional effects including neuronal differentiation, neuroprotection and axon elongation. In this study, I investigated whether resveratrol induces neuronal differentiation of human bone marrow derived mesenchymal stem cells (hBM-MSCs). Quantitative PCR results showed that resveratrol-treated MSCs (RSV-MSCs) have significantly increased expression of the neuropro-genitor markers *Nestin*, *Musashi*, *CD133* and *GFAP*. When RSV-MSCs were differentiated with neuronal induction media (RSV-dMSCs), they exhibited a cell body and dendritic morphology similar to neurons. The number and

neurite length of these RSV-dMSCs were significantly increased compared to differentiated MSCs (dMSCs). Both RSV-dMSCs and dMSCs have significantly increased expression of the neuronal-specific marker genes *Nestin*, *Musashi*, *CD133*, *GFAP*, *NF-M*, *MAP-2* and *KCNH1*. The RSV-dMSCs also showed a increased expression of the neuronal marker proteins, Nestin and NF-M, based on immunocytochemical staining and immunoblot analysis. These effects were abolished by the treatment of SIRT1 inhibitor EX527. Therefore, I have shown that resveratrol treatment, along with the use of neuronal induction media, effectively stimulates neuronal cell differentiation of hBM-MSCs.

Next, I investigated whether rolipram, phosphodiesterase 4 (PDE4) inhibiotr, induces neuronal differentiation of human bone marrow mesenchymal stem cells (hBM-MSCs). Rolipram-treated MSCs (Roli-MSCs) have significantly increased expression of the neuroprogenitor proteins Nestin, Musashi, GFAP and Sox-2. When Roli-MSCs were differentiated with neuronal induction media (Roli-dMSCs), they exhibited cell body and dendritic morphologies similar to those of neurons. The neurite number and length of Roli-dMSCs were significantly increased compared to those of differentiated MSCs (dMSCs). Compared with undifferentiated hBM-MSCs, the Roli-dMSCs and dMSCs showed significantly increased expression of the neuronal-specific marker genes, *Nestin*, *Musashi*, *CD133*, *GFAP*, *NF-M*, *MAP-2*, *KCNH1* and *KCNH5*, and decreased expression of other lineage-specific markers *Adiponectin*, *FABP4*, *MMP13* and *ALP*. The Roli-dMSCs also showed a

higher expression of the neuronal marker proteins Nestin, Musashi, Sox-2, NF-M and Tuj-1 compared to those of the undifferentiated hBM-MSCs, based on immunocytochemical staining and immunoblot analysis. Thus, I have shown that rolipram promotes neuronal differentiation by the induction of neuroprogenitor expression in hBM-MSCs.

Therefore, SIRT1 activators in hBM-MSCs may induce to neuronal differentiaton and improve the therapeutic efficacy of stem cell therapy for neurodegenerative disorders.

국문 초록

인간의 골수 유래 중간엽 줄기세포에서 SIRT1 활성제를 통한 신경분화 촉진

인간의 중간엽 줄기세포(hMSCs)는 신경세포로 분화할 수 있는 특징을 가져, 퇴행성 신경계질환을 치료하는데 도움을 준다고 알려졌다. 이를 치료목적으로 이용할 경우, 줄기세포의 분화능은 치료의 효율성에 결정적인 영향을 미치는 요인 중 하나이다. 최근 연구들에 의하면, sirtuin1 (SIRT1)의 활성은 신경분화, 신경보호 효과, 축삭돌기의 신장에 효과가 있다고 알려졌다. 본 연구에서는 먼저, 인간의 골수 유래 중간엽 줄기세포(hBM-MSCs)에서 resveratrol (RSV)이 신경분화를 효율적으로 유도하는지 확인해 보고자 하였다. quantitative PCR (qPCR)을 통해, 줄기세포 배양 배지에 RSV과 함께 배양한 세포(RSV-MSCs)는 control-MSCs (Ctrl-MSCs)와 비교하여 신경 전구체 마커인 *Nestin*, *Musashi*, *CD133*, *GFAP*의 발현량이 증가하는 것을 확인하였다. RSV을 전 처리한 뒤, 분화유도 배양액으로 신경세포분화(RSV-dMSCs)를 유도했을 때, 전 처리 되지 않은 줄기세포로부터 분화된 신경세포(dMSCs)에 비해 분화율과 신경돌기의 길이 및 수에서 상당히 증가함을 보였다. qPCR을 통해 신경 전구체 마커인 *Nestin*, *Musashi*, *CD133*, *GFAP*와 신경 특이적 마커인 *NF-M*, *MAP-2*, *KCNH1*을 확인해본 결과 상당한 증가폭을 나타내었다. 또한, immunocytochemical staining과 immunoblot analysis를 통해 RSV-dMSCs에서 Nestin, NF-M이 높은 수준으로 발현하는 것을 확인하였다. 이러한 효과는 SIRT1의 억제제인 EX527을 중간엽 줄기세포에 처리한 결과 억제됨을 확인하

였다. 그러므로 RSV 전처리 이후 신경분화 유도 시, 인간의 골수 유래 중간엽 줄기세포의 신경분화에 효과적으로 자극될 수 있음을 보여준다.

다음으로 phosphodiesterase 4 (PDE4)를 억제하는 rolipram이 인간의 골수 유래 중간엽 줄기세포에서 신경분화를 효과적으로 유도하는지 확인해 보고자 하였다. 줄기세포 배양 배지에 rolipram을 처리하여 배양한 세포(Roli-MSCs)를 qPCR을 통해 신경 전구체 마커인 *Nestin*, *Musashi*, *CD133*, *GFAP*의 발현을 확인해본 결과 상당히 증가하는 것을 확인하였고, immunoblot analysis를 통해 신경전구체 마커인 Nestin, Musashi, GFAP, Sox-2의 단백질이 높은 수준으로 증가하는 것을 확인하였다. Rolipram을 전 처리 한 뒤, 분화유도 배양액으로 신경세포로의 분화(Roli-dMSCs)를 유도했을 때, 전 처리 되지 않은 줄기세포로부터 분화된 신경세포(dMSCs)에 비해 분화율과 신경돌기의 길이 및 수에서 상당한 차이를 보였다. qPCR을 통해 신경전구체 마커 *Nestin*, *Musashi*, *CD133*, *GFAP*와 신경 특이적 마커인 *NF-M*, *MAP-2*, *KCNH1*, *KCNH5*에서 상당한 증가 양상을 보이는 것을 확인하였고, 다른 계통의 특이적 마커인 *Adiponectin*, *FABP4*, *MMP13*, *ALP*의 발현은 감소하였다. 또한, immunocytochemical staining과 immunoblot analysis를 통해, Roli-dMSCs에서 Nestin, Musashi, Sox-2, NF-M, Tuj-1의 수준이 상당히 증가함을 확인하였다. 그러므로 인간의 골수 유래 중간엽 줄기세포에 rolipram 전처리 후 신경분화를 유도할 경우 그 효과가 증진되는 것을 확인하였다.

따라서 SIRT1 활성제를 전 처리한 뒤 신경 분화를 유도할 경우, 퇴행성 신경계질환의 줄기세포 치료제로써 치료적 효능이 있음을 제시한다.

INTRODUCTION

Human bone marrow mesenchymal stem cells (hBM-MSCs) are characterized by their multipotency to differentiate into diverse cell lineages [21] including neuron-like cells [16,29], which have been used for cell therapy in neurodegenerative diseases [3]. However, human MSCs have a poor neuronal differentiation rate when engrafted, which limits their therapeutic efficacy [8].

Sirtuin1 (SIRT1) have been categorized as an NAD^+-dependent class III histone deacetylases (HDACs) [5]. SIRT1 activation is associated with protein deacetylation of nuclear histone, transcription factors, and cell-signaling mediators [5], resulting in the alteration of cellular signaling and gene expression of anti-senescence, cellular protection, and neuronal differentiation [5,9,11,12,17,19]. Also, there is increasing evidence that SIRT1 activation has an important effect on neuronal architecture by stimulating axon elongation [17] and neurite outgrowth [9,26].

Resveratrol-3,4,5-trihydroxy-trans-stillbene (resveratrol; RSV), a natural non-flavonoid polyphenol compound, provides protection against stress injury, excessive sunlight, ultraviolet radiation, infections, and invading fungi [24]. There is increasing evidence that resveratrol plays a pivotal role in neuroprotection [5,11,19] and neuronal differentiation [9,17]. Most of these beneficial effects by resveratrol are dependent on SIRT1 activation [5,11,19], although resveratrol indirectly activates SIRT1 by increasing intracellular

cAMP following the inhibition of cAMP-dependent phosphodiesterase (PDE) [20].

Rolipram, which up-regulates intracellular cAMP through blocking phosphodiesterase 4 (PDE4) enzyme activity, can mitigate diverse neurological disorders. Increased intracellular cAMP can promote axonal elongation [33, 34] and facilitate neuronal repair [35,36], while decreased cAMP is associated with losses in neuronal regenerative capacity [37]. Also, rolipram reproduces the metabolic effects of resveratrol including activation of AMPK and increase of NAD^+ levels, which supports SIRT1 activation [20].

Since SIRT1 activation has been reported to induce the neuronal differentiation [9,17] and has beneficial effects in neurodegenerative diseases [5,11], I investigated whether the SIRT1 activators, resveratrol and rolipram can promote neuronal differentiation in hBM-MSCs.

Part I. Resveratrol-induced SIRT1 activation promotes neuronal differentiation of human bone marrow mesenchymal stem cells

I. Introduction

Human mesenchymal stem cells (hMSCs) are classically defined as multipotent cells, which can differentiate into diverse cell types, including bone, cartilage, fat, tendon, muscle, and marrow stroma [2,21]. Recent studies have shown that hMSCs can also differentiate into neuron-like cells [16,53]. There is an increasing interest in the use of hMSCs in regenerative medicine for neurodegenerative diseases [3]. However, most of the engrafted cells die within a week after transplantation [8] and only a few cells successfully differentiate into neurons and are engrafted into injured tissues, which severely limits the efficacy of the therapy [8]. Although researchers differentiate the stem cells into neurons prior to engrafting into patients with neurodegenerative diseases, many stem cells die during the progress of neuronal differentiation. Thus, the rate of differentiation prior to application in cell therapy needs to be improved.

Resveratrol-3,4,5-trihydroxy-trans-stillbene (resveratrol; RSV), a natural non-flavonoid polyphenol compound, has been obtained from various plants, including grapes, peanuts, pine trees and cassia, and many food products [23]. Resveratrol has been widely used for over several decades as a

defense agent against stress injury, excessive sunlight, ultraviolet radiation, infections, and invading fungi [24]. Most of these beneficial effects by resveratrol are dependent on sirtuin1 (SIRT1) activation [5,11,19], although resveratrol indirectly activates SIRT1 by increasing intracellular cAMP following the inhibition of cAMP-dependent phosphodiesterase (PDE) [20].

Recent studies have shown that SIRT1 activation plays a pivotal role in neurodegenerative diseases and brain senescence because its neuro-protective effects correlated with its functions in metabolism, stress resistance and genomic stability [11]. SIRT1 also affects microtubule dynamics during axon elongation by deacetylating AKT and interacting with mircroRNA [17]. Cytoplasmic SIRT1 down-regulates mTOR and stimulates neurite outgrowth [9,26], which indicates the role of SIRT1 in neuronal differentiation and the structural features of neuronal cells. Therefore, these previous reports suggest that SIRT1 activation may be important for the induction of neuronal differentiation.

Since SIRT1 activation has been reported to induce the neuronal differentiation [9,17] and has beneficial effects in neurodegenerative diseases [5,11], I investigated whether the SIRT1 activator resveratrol stimulates neuronal differentiation through the induction of neuroprogenitor genes in hBM-MSCs.

II. Materials and Methods

II-1. Characteristics of primary hBM-MSCs and cell culture

The hBM-MSCs were purchased from CEFO (Cell Engineering for Origin; Seoul, Korea). The cells were examined for viral infection and mycoplasma contamination, and all were presented as negative. Flow cytometric analysis of the cells revealed a $CD73^{+}$, $CD105^{+}$, and $CD31^{-}$. phenotype. The hBM-MSCs were cultured in T75 flasks (Becton Dickinson; San Jose, CA, USA) according to the manufacturer's recommendations. Cells were cultured in hBM-MSC growth medium (DMEM; Gibco; Grand Island, NY, USA), containing 10% fetal bovine serum (FBS), L-glutamine, penicillin, and streptomycin, without any stimulatory supplements or vitamins. Cells were maintained in a humidified incubator at 37 °C, using a standard mixture of 95% air and 5% CO_2. hBM-MSCs at passage seven were used in this study.

II-2. Quantitative PCR (qPCR)

hBM-MSCs were harvested and total RNA was extracted using RNAiso reagent (TaKaRa Bio; Shiga, Japan) according to the manufacturer's instructions. The Primescript™ II 1st strand cDNA synthesis kit (TaKaRa Bio; Shiga, Japan) was used to reverse transcribe 3–5 μg of total RNA with 5 μ

M of Oligo (dT) primers (TaKaRa Bio; Shiga, Japan), 1 mM each dNTP, and the supplied buffer. cDNA was amplified using Power SYBR® Green PCR master mix (Applied Biosystems Inc., Waltham, MA, USA) with gene-specific primers for human *Nestin*, *Musashi*, *CD133*, *GFAP*, *MAP-2*, *NF-M*, *KCNH1*, *ANG*, *VEGF*, *ALP*, *Adiponectin*, *FABP4*, *MMP13* or *β-actin*. The real-time PCR cycling parameters were as follows: 95 °C for 10 min, followed by 40 cycles of 15 s at 95 °C, and 1 min at 60 °C. The primers were synthesized by GenoTech (GenoTech Corp.; Daejeon, South Korea) and IDT (Integrated DNA Technologies Inc.; Coralville, IA, USA) and are summarized in Table 1.

Table 1. Oligonucleotides used for real-time PCR.

Gene	Forward primer (5' → 3')	Reverse primer (5' → 3')	Acc. No.
Nestin	AGCCCTGACCACTCCAGTTT	GCTGCTTACCACTTTGCCCT	NM_006617
Musashi	ATAAAGTGCTGGCGCAATCG	TCGTTCGAGTCACCATCTTGG	NM_002442
CD133	CCTGGGGCTGCTGTTTATTAT	ATTTTCCTTCTGTCGCTGGT	NM_006017
GFAP	TGGGAGCTTGATTCTCAGCA	CCTGGGCTTGACCTCTCTGTA	NM_002055
MAP-2	TTGGTGCCGAGTGAGAAGAA	GGTCTGGCAGTGGTTGGTTAA	NM_002374
NF-M	GTGAACCACGAGAAGGCTCA	AGGTAGTCTTTGCGCTCCAC	NM_005382
KCNH1	TTGGAGATGTGTTCTGGAAGGAA	AGGGCATCCCGCTTGATC	NM_172362.2
ANG	ATGGTGATGGGCCTGGGCGT	CAGTCAATTTTCCGTCGTCCGTA	NM_001145
VEGF	AGAAAATCCCTGTGGGCCTT	GTCACATCTGCAAGTACGTTCG	NM_001025368
ALP	GCACCATGAAGGAAAAGCCA	TGTGAAGACGTGGGAATGGT	NM_000478
Adiponectin	ACATGCCCATTCGCTTTACC	AGAGGCTGACCTTCACATCC	NM_001177800
FABP4	GGCATGGCCAAACCTAACAT	CCTGGCCCAGTATGAAGGAA	NM_001442
MMP13	TTCCCAGTGGTGGTGATGAA	CAGGATTCCCGCGAGATTTG	NM_002427
β-actin	ATCCGCAAAGACCTGTACGC	TCTTCATTGTGCTGGGTGCC	NM_001101

Acc. No. indicates gene access number.

II-3. (4,5-Dimethylthiazol-2-yl-) 2,5-diphenyltetrazolium bromide (MTT) assay

The cell viabilities of resveratrol-treated MSCs were evaluated by MTT assay (Sigma-Aldrich; St. Louis, MO, USA) performed according to the manufacturer's instructions. Briefly, 2.5 × 10^3 hBM-MSCs were seeded onto 96-well plates. The next day, the cells were incubated with 0–50 μM of resveratrol for 12 h and subjected to MTT assay.

II-4. Neuronal differentiation

hBM-MSCs were incubated with/without 1 μM resveratrol for 12 h. The cells were then exposed to pre-induction media containing DMEM, 10% FBS, 10 ng/mL basic fivrovlast growth factor, and 500 μM β-mercaptoethanol for 24 h. The media was replaced with induction media containing 100 μM butylated hydroxyanisole (BHA) and 2% dimethyl sulfoxide (DMSO) in FBS-free media for 6 h, according to previously described procedures [16]. Control-MSCs were incubated with FBS-containing media for 24 h. The media were replaced with FBS-free media and the cells were further incubated for 6 h. Images were captured with a microscope (Eclipse TS100, Nikon, Tokyo, Japan) and a digital camera (i-Solution IMTcam3; JENOPTIK, Jena, Germany). Neurite lengths were measured using the Image J program (NIH, Bethesda, MD, USA).

II-5 Immunocytochemical staining

hBM-MSCs were grown on poly-L-lysine-coated coverslips (Fisher Scientific, Hampton, NH, USA) and induced to differentiate into neuron-like cells. Cells were then subjected to immunocytochemical staining with antibodies against NF-M or Nestin (Santa Cruz biotechnology, Dallas, TX, USA) diluted 1:200 in blocking buffer overnight at 4 °C, and subsequently, Alexa Fluor® 488-conjugated donkey anti-goat IgG secondary antibodies (Molecular Probes Inc., Carlsbad, CA, USA) diluted 1:500 in Hoechst 33342 (Molecular Probes Inc., Carlsbad, CA, USA) for 1 h at RT. The cells were visualized by fluorescence microscopy with a Nikon Eclipse 80Ti microscope (Nikon; Tokyo, Japan). Cell images were taken with a DS-RI1 digital camera (Nikon; Tokyo, Japan).

II-6. Immunoblot analysis

Cells were extracted with 400 μl radioimmunoprecipitation assay buffer containing protease and phosphatase inhibitors (Santa Cruz Biotechnology; Dallas, TX, US) for 30 min at 4 °C and then centrifuged at 16,000 × *g* for 20 min. Total protein was then subjected to immunoblotting with antibodies against NF-M (1:500), Nestin (1:500) or β-actin (1:5000), and subsequently, the appropriate horseradish peroxidase-conjugated secondary antibodies (1:10,000; Jackson Immuno Research Laboratories; West Grove, PA, U.S.A).

The bands were quantified with the Image J program (NIH, USA).

II-7. Statistical analysis

The data are represented as mean ± standard deviation (SD) of three or more independent experiments. Statistical comparisons between groups were made using an independent *t*-test. p-Values < 0.05 were considered statistically significant.

III. Results

III-1. Neuroprogenitor gene markers are induced by resveratrol in hBM-MSCs

To evaluate the effects of resveratrol (RSV), hBM-MSCs were incubated with 0–10 μM of resveratrol for 4 h. The expression of neuroprogenitor markers, *Nestin* and *Musashi*, were assessed by qPCR. As shown in Fig. 1A, the maximum expressions were obtained after incubation with 1 μM RSV (Fig. 1A; *t*-test, $*p < 0.05$, mean ± SD, n=3). To determine the optimal time of RSV incubation in hBM-MSCs, MSCs were incubated with 1 μM for several times (0–24 h). Expression of the tested genes maximized after incubation for 12 h (Fig. 1B; *t*-test, $*p < 0.05$, $\#p < 0.005$, mean ± SD, n=4). Cellular toxicities were not observed for up to 50 μM RSV for 12 h (Fig. 1C; mean ± SD, n=3). From these data, we determined that 1 μM RSV for 12 h was the optimal treatment condition. We have shown that RSV stimulates the expression of neuroprogenitor genes under the optimized condition (Fig. 1A–C). To further evaluate the role of RSV in cell fate, additional neuroprogenitor genes were measured by qPCR. The expression of neuroprogenitor genes, *Nestin*, *Musashi*, *CD133* and *GFAP*, was significantly increased in resveratrol-treated hBM-MSCs (RSV-MSCs) while *ANG* and *VEGF* levels were unchanged compared to the non-treated hBM-MSCs (Fig. 1D; *t*-test, $*p < 0.05$, mean ± SD, n = 4).

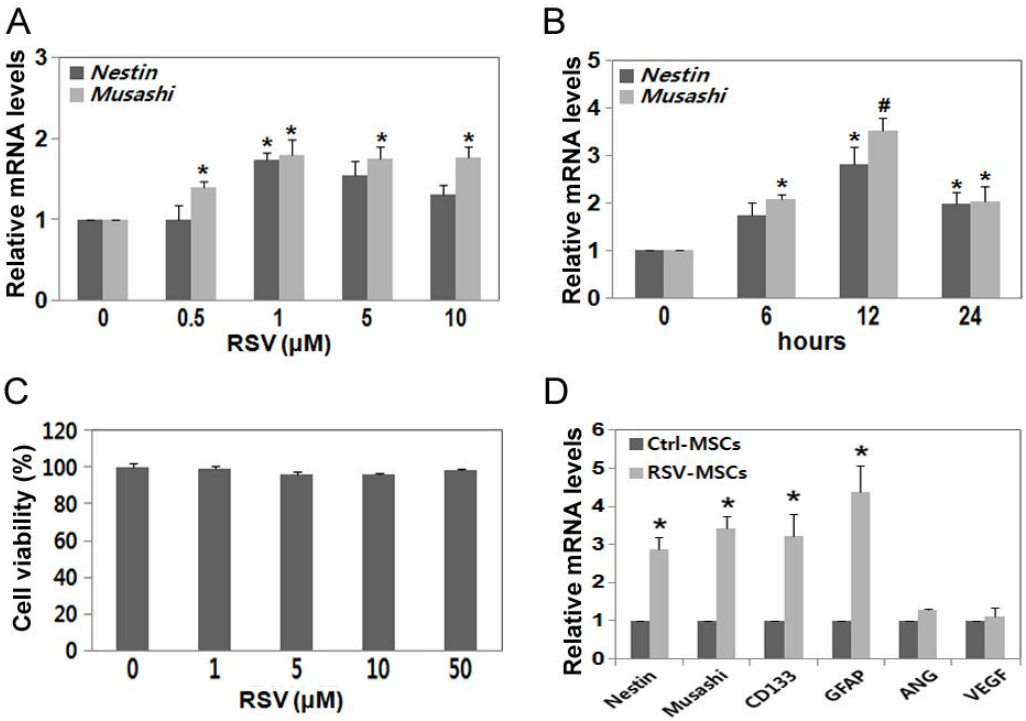

Figure 1. Resveratrol induces the expression of neuroprogenitor markers in hBM-MSCs.

(A) hBM-MSCs were treated with 0–10 μM of RSV for 4 h. The expression of the neuroprogenitor genes *Nestin* and *Musashi* was identified by qPCR. (B) 1 μM RSV was applied for various incubation times (0–24 h), then *Nestin* and *Musashi* were measured by qPCR. (C) Cytotoxicities were estimated for several concentrations (0–50 μM) of resveratrol-treated MSCs (RSV-MSCs). (D) MSCs were treated with 1 μM RSV for 12 h (pre-determined conditions) and the gene expressions were measured by qPCR. The neuroprogenitor markers, *Nestin*, *Musashi*, *CD133* and *GFAP*, were significantly increased in RSV-MSCs compared to non-treated hBM-MSCs (Ctrl-MSCs).

III-2. Resveratrol-pretreated hBM-MSCs have a neuronal appearance in neuronal induction media

Since resveratrol stimulates the expression of neuroprogenitor genes, I hypothesized that RSV-MSCs could be more effectively differentiated into neuronal cells than control MSCs (Ctrl-MSCs). To evaluate this hypothesis, both MSCs (Ctrl- and RSV-MSCs) were differentiated with neuronal induction media [16]. Both neuronal differentiated MSCs (Fig. 2A; dMSCs and RSV-dMSCs) exhibited neuronal morphology, while undifferentiated Ctrl-MSCs and RSV-MSCs showed a flattened and spindle-shaped appearance similar to primary hBM-MSCs (Fig. 2A, Ctrl-MSCs and RSV-MSCs). Cells were considered as neuronal differentiated cells when each cell body had more than two dendrites longer than 60 μm. According to the rate of neuronal differentiation in RSV-dMSCs and dMSCs, a higher percentage of RSV-dMSCs significantly differentiated into neuron-like cells compared to dMSCs (Fig. 2B; *t*-test, #$p < 0.01$, mean ± SD, n=4). The average neurite length of dMSCs was also significantly greater in RSV-dMSCs (Fig. 2C; *t*-test, *$p < 0.05$; mean ± SD, n=4). However, a significant difference in the number of neurites was not observed for dMSCs or RSV-dMSCs (Fig. 2D).

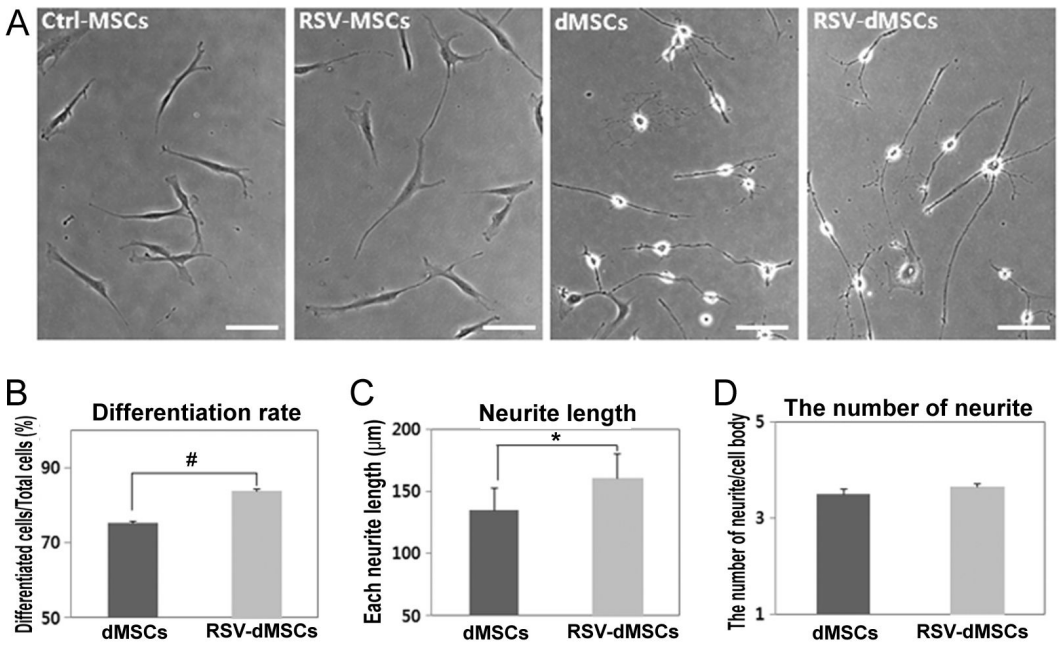

Figure 2. Neuron-like morphological changes in RSV-pretreated BM-MSCs followed by neuronal induction.

(A) Both Ctrl-MSCs and RSV-MSCs were differentiated into neuronal cells following exposure to neuronal induction media. Differentiated MSCs are shown in dMSCs and RSV-dMSCs. Scale bar indicates 100 μm. (B) Total cells and neuronal-shaped cells were counted to estimate the neuronal differentiated rate. RSV-dMSCs were significantly differentiated compared to dMSCs. (C) The neurite length of differentiated cells was significantly longer in RSV-dMSCs. (D) The number of neurites in differentiated cells did not significantly increase.

Table 2. The neuronal-like cells were counted to estimate the neuronal differentiation rate.

Experiments (n=3)	dMSCs (Differentiated cells/total cells)	RSV-dMSCs (Differentiated cells/total cells)
1st	637 / 838	914 / 1083
2nd	715 / 968	927 / 1120
3rd	627 / 828	736 / 872
Sum	1979 / 2634 (75.1%)	2577 / 3075 (83.8%)

Table 3. The number of neurites from each differentiated cells were counted and neurite lengths were measured.

dMSCs			
Experiments (n=4)	**Total cells**	**The No. of Neurite (Ave/each cell)**	**Neurite length (Ave/each neurite, ㎛)**
1st	105	3.32	86.13
2nd	75	3.46	154.67
3rd	60	3.47	130.27
4th	112	3.78	169.00
Ave.	88	3.51	135.02

RSV-dMSCs			
Experiments (n=4)	**Total cells**	**The No. of Neurite (Ave/each cell)**	**Neurite length (Ave/each neurite, ㎛)**
1st	105	3.64	108.91
2nd	75	3.59	166.86
3rd	60	3.55	162.81
4th	112	3.82	204.90
Ave.	88	3.65	160.87

III-3. Significant increases in the expression of diverse neuronal markers in resveratrol-dMSCs

Since RSV-dMSCs have a neuronal appearance, the expression of various neuronal-specific marker genes was evaluated by qPCR (Fig. 3A). All genes tested in this study were significantly increased in either RSV-dMSCs or dMSCs compared to the Ctrl-MSCs (Fig. 3A; *t*-test, $*p < 0.001$, mean ± SD, n=4). The expression of neuronal-specific marker genes, *Nestin*, *Musashi*, *CD133* and *MAP-2*, was significantly increased in RSV-dMSCs compared to that of dMSCs (Fig. 3A; *t*-test, $*p < 0.05$, $\#p < 0.05$, mean ± SD, n=4). I also examined the expression of other lineage specific markers in dMSCs and RSV-dMSCs, and identified decreased expression of osteogenic (*ALP*), adipogenic (*Adiponectin*, *FABP4*) and chondrogenic (*MMP13*) specific genes in dMSCs and RSV-dMSCs compared to the Ctrl-MSCs (Fig. 3B; mean ± SD, n=3).

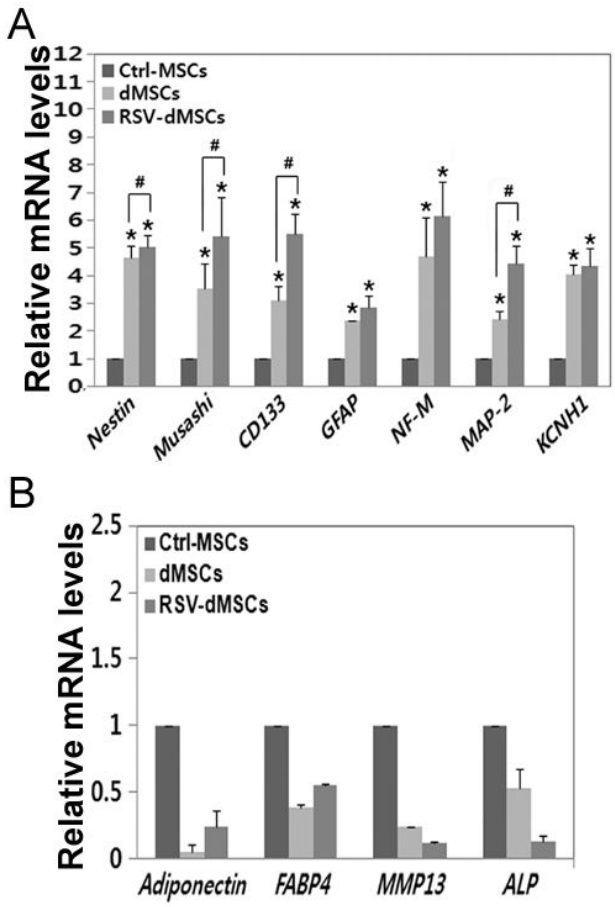

Figure 3. Diverse neuronal markers are increased in differentiated RSV-MSCs.

(A) The expression of several neuronal specific genes were measured in MSCs (Ctrl-MSCs) and differentiated MSCs (dMSCs, RSV-dMSCs) by qPCR. All genes tested in this experiment were significantly increased in differentiated MSCs. *Musashi*, *CD133*, *Nestin* and *MAP-2* were significantly increased in RSV-dMSCs compared to dMSCs. (B) The expressions of osteogenic, adipogenic and chondrogenic specific genes were decreased in both dMSCs and RSV-dMSCs compared to Ctrl-MSCs.

III-4. Neuronal-specific proteins are up-regulated in resveratrol-dMSCs

To characterize whether neuronal differentiation was observed at the protein level, I used immunocytochemical staining. Ctrl-MSCs, dMSCs and RSV-dMSCs were fixed and stained with specific antibodies against the neuronal marker proteins NF-M and Nestin. Neuronal-induced MSCs (dMSCs) and RSV-dMSCs exhibited positive cytoplasmic staining for both NF-M and Nestin compared to the non-induced MSCs (Ctrl-MSCs, Fig. 4A). Similar results were obtained from immunoblot analysis using antibodies specific to NF-M and Nestin (Fig. 4B). Most of the beneficial effects by resveratrol were achieved through SIRT1 activation [5,11,19]. To evaluate whether these resveratrol effects are induced through SIRT1 activation, the SIRT1-specific inhibitor EX527 was used. MSCs were induced with neuronal differentiation media followed by incubation with EX527 (10 μM for 24 h) [22,25] and then subjected to immunocytochemical staining and immunoblot analysis. As shown in Fig. 4, neuronal-specific marker proteins Nestin and NF-M were down-regulated in EX527-treated MSCs (EX-MSCs).

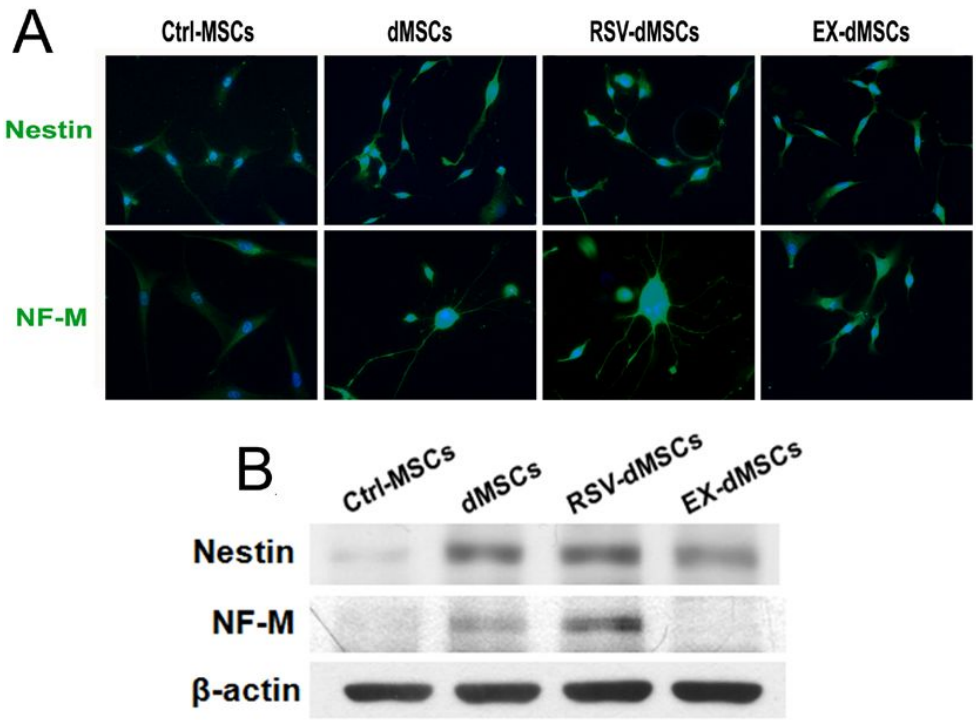

Figure 4. Up-regulation of neuronal-specific proteins in RSV-dMSCs.

(A) MSCs (Ctrl-MSCs) and differentiated MSCs (dMSCs, RSV-dMSCs and EX-dMSCs) were fixed and stained with antibodies for specific neuronal markers Nestin (upper panel) and NF-M (lower panel), and visualized by fluorescent microscopy. (B) The MSCs were subjected to immunoblot analysis with antibodies for NF-M and Nestin. β-actin was used as an internal standard.

IV. Discussion

Resveratrol is an anti-aging natural compound [23] that increases the life span in several species [1,13,18,28]. Recent studies have demonstrated that resveratrol plays a pivotal role in neuroprotection [5,11,19] and neuronal differentiation [9,17]. In this study, I investigated whether resveratrol induces neuronal differentiation of hBM-MSCs. MSCs were treated with 1 μM resveratrol for 12 h, which is the optimized condition from this study (Fig. 1A and B). Results showed increased expression of the neuronal progenitor genes *Nestin*, *Musashi*, *CD133* and *GFAP* (Fig. 1D), suggesting that resveratrol treatment stimulates neuronal differentiation in hBM-MSCs. To further evaluate the effects of resveratrol on neuronal differentiation, resveratrol-pretreated MSCs (RSV-MSCs) were cultured with neuronal induction media [16]. Here, I have shown that hBM-MSCs effectively differentiate into neuron-like cells following resveratrol treatment, and that there is significant increase in the differentiation rate of RSV-dMSCs (Fig. 2A and B).

There is increasing evidence that SIRT1 activation has an important effect on neuronal architecture by stimulating axon elongation [17] and neurite outgrowth [9,26]. In this study, neurite lengths were also significantly longer in RSV-dMSCs (Fig. 2C). These cells had significantly increased expression of all neuronal-specific markers (Fig. 3A; *Nestin*, *Musashi*, *CD133*, *GFAP*, *MAP-2*, *NF-M* and *KCNH1*), and decreased expression of other lineage-specific markers (Fig. 3B; *ALP*, *Adiponectin*, *FABP4*, *MMP13*) in both differentiate dMSCs. The gene expressions of *MAP-2* (dendritic marker),

Musashi, *Nestin* and *CD133* were significantly increased in RSV-dMSCs compared to dMSCs (Fig. 3). This suggests that RSV-MSCs were more effectively differentiated into neuron-like cells than the Ctrl-MSCs in the presence of neuronal induction media.

SIRT1 activation is associated with protein deacetylation of nuclear histone, transcription factors and cell signaling mediators [5], resulting in the alteration of cellular signaling and gene expression of anti-senescence, cellular protection and neuronal differentiation [5,9,11,12,17,19]. SIRT1 activation by resveratrol is reversible in these functional activities. The withdrawal of resveratrol may return these proteins back to their acetylated form. This suggests that the timing of SIRT1 activator treatment is critical for inducing effective cell differentiation. In this study, I found resveratrol pre-incubation prior to neuronal induction effectively induces neuronal differentiation by the expression of neuroprogenitor markers in hBM-MSCs (Fig. 1 and 2). The neuronal differentiate dMSCs (dMSCs) were confirmed with neuronal specific markers, using immunocytochemical staining and immunoblot analysis with antibodies targeting NF-M and Nestin proteins. The up-regulation of these proteins was observed for both neuronal differentiated MSCs and RSV-pretreated MSCs (Fig. 4).

Although a recent study has shown that resveratrol directly inhibits cAMP-dependent phosphodiesterase (PDE) activity and indirectly activates SIRT1 through a signaling cascade involving cAMP, Epac1 and AMP-activated protein kinase (AMPK) [20], it is well known that the beneficial effects of

resveratrol are achieved through SIRT1 activation [5,11,19]. Here, I examined whether neuronal differentiation by resveratrol is induced through SIRT1 activation. BM-MSCs were pretreated with SIRT1-specific inhibitor EX527 [22,25] and then incubated with neuronal induction media. I have identified a large decrease in the expression of neuronal marker proteins, Nestin and NF-M, by immunocytochemical and immunoblot analysis (Fig. 4), suggesting that resveratrol promotes neuronal differentiation through SIRT1 activation in hMSCs.

I have shown that resveratrol pretreatment of hBM-MSCs effectively stimulates neuronal differentiation. However, the signaling pathways that are directly involved in this process have not been confirmed. Based on the functional mechanism of resveratrol as a SIRT1 activator, resveratrol induces protein deacetylation, resulting in the modulation of several signaling pathways [27] and gene expressions [14]. Since resveratrol has been shown to have positive effects in preclinical studies in neurological disease models [4,6,7,10,11,15], some resveratrol-induced modifications may be functionally active in stem cell differentiation, especially neuronal differentiation. Previous studies showing that SIRT1 activation enhances the differentiation capacity of stem cells [5,9,11,17,26] also support our results.

BM-MSCs, which have the potential to differentiate into neurons [16], have been used for stem cell therapy in neurodegenerative diseases [3]. However, only a few cells among the transplant dMSCs were differentiated into neuronal cells in an in vivo study [8]. This suggests that the differentiation

potency of stem cells needs to be improved prior to implantation. In this study, I have shown that resveratrol promotes neuronal differentiation by the induction of neuroprogenitor genes in hBM-MSCs, and suggest that resveratrol pretreatment of MSCs may be beneficial in cell therapy for neurodegenerative diseases.

This study has demonstrated that resveratrol-treated MSCs endogenously induce the expression of neuroprogenitor marker genes that synergistically promote neuronal differentiation in the presence of neuronal induction media. Thus, resveratrol-pretreated MSCs may enhance neuronal differentiation and provide advances in stem cell therapy for neurodegenerative disorders.

Part II. PDE4 inhibition by rolipram promotes neuronal differentiation in human bone marrow mesenchymal stem cells

I. Introduction

Human bone marrow-mesenchymal stem cells (hBM-MSCs) are characterized by their multipotency to differentiate into diverse cell lineages [21] including neuron-like cells [16,29]. MSCs are easily isolated from human bone marrow, fat and umbilical cord tissues [2], and can be expanded by in vitro culture to secure a sufficiently high number of cells for use in clinical applications. Thus, MSCs have been used in regenerative medical therapies for neurodegenerative disorders such as amyotrophic lateral sclerosis [30], Parkinson's disease [31] and stroke [32]. However, MSCs have a poor neuronal differentiation rate when engrafted, which limits their therapeutic efficacy [8].

Recent studies have shown that an increased level of intracellular cyclic adenosine monophosphate (cAMP) can promote axonal regeneration [33,34] and facilitate neuronal repair [35,36], while a decreased level of intracellular cAMP is associated with losses in neuronal regenerative capacity [37]. It has been reported that cAMP promotes neuronal differentiation through up-regulating the expression levels of the neuronal markers NSE, Tuj1 and GFAP [38]. A cAMP-hydrolyzing enzyme, phosphodiesterase-4 (PDE4), which

is a key regulator of the levels of intracellular cAMP, hydrolyzes cAMP to 5'-AMP, resulting in a decrease in the intracellular cAMP level. PDE4 inhibition has been shown to improve depression, cognitive faculty [16] and Alzheimer's disease [40], while PDE4B-deficient animals presented an anti-psychotic phenotype [41].

A selective PDE4 inhibitor, rolipram, has been developed as a potential anti-depressant drug [42]. It has been widely examined in several disease models, including autoimmune diseases [43], Alzheimer's disease [40,44], cognitive enhancement [53], Huntington's disease [45], traumatic brain injury (TBI) [46], spinal cord injury [47] and respiratory diseases [48], and has been identified to have beneficial effects in these disease models. Interestingly, recent studies have shown that resveratrol, which ameliorates aging-related metabolic phenotypes and neuronal degeneration, also inhibits PDE4, leading to an increased level of cAMP [20].

Since modulation of cAMP has been associated with axonal elongation and neuronal regeneration [33-36], and has shown beneficial effects in neurological diseases [39-41], I investigated whether the PDE4 inhibitor rolipram can promote neuronal differentiation in hBM-MSCs.

II. Materials and Methods

II-1. Characteristics of primary hBM-MSCs and cell culture

The hBM-MSCs were purchased from CEFO (Cell Engineering for Origin, Seoul, Korea). The cells were examined for viral infection and mycoplasma contamination, and presented as negative. Flow cytometric analysis of the cells revealed a $CD73^+$, $CD105^+$ and $CD31^-$ phenotype. The hBM-MSCs were cultured in T75 flasks (Becton Dickinson, San Jose, CA, USA) according to the manufacturer's recommendations. Cells were cultured in hBM-MSC growth medium (DMEM; Gibco, Grand Island, NY, USA), containing 10% (v/v) fetal bovine serum (FBS), L-glutamine, penicillin, and streptomycin, without any stimulatory supplements or vitamins. Cells were maintained in a humidified incubator at 37 °C, using a standard mixture of 95% air and 5% CO_2. Cells at passage 7 were used in this study.

II-2. Quantitative PCR (qPCR)

hBM-MSCs were harvested and total RNA was extracted using RNAiso reagent (TaKaRa Bio, Shiga, Japan) according to the manufacturer's instructions. The Primescript™ II 1st strand cDNA synthesis kit (TaKaRa Bio) was used to reverse transcribe 3–5 μg of total RNA with 5 μM of Oligo (dT) primers (TaKaRa Bio), 1 mM each dNTP and the supplied buffer. cDNA was

amplified using Power SYBR® Green PCR master mix (Applied Biosystems Inc., Waltham, MA, USA) with gene-specific primers for human *Nestin*, *Musashi*, *CD133*, *GFAP*, *MAP-2*, *NF-M*, *KCNH1*, *KCNH5*, *Nanog*, *Oct-4*, *ALP*, *Adiponectin*, *FABP4*, *MMP13* or *β-actin*. The real-time PCR cycling parameters were as follows: 95 °C for 10 min, followed by 40 cycles of 15s at 95 °C and 1 min at 60 °C. The primers were synthesized by GenoTech (GenoTech Corp., Daejeon, South Korea) and IDT (Integrated DNA Technologies Inc., Coralville, IA, USA) and are summarized in Table 1.

Table 1. Oligonucleotides used for real-time PCR.

Gene	Forward primer (5' à 3')	Reverse primer (5' à 3')	Acc. No.
Nestin	AGCCCTGACCACTCCAGTTT	GCTGCTTACCACTTTGCCCT	NM_006617
Musashi	ATAAAGTGCTGGCGCAATCG	TCGTTCGAGTCACCATCTTGG	NM_002442
CD133	CCTGGGGCTGCTGTTTATTAT	ATTTTCCTTCTGTCGCTGGT	NM_006017
GFAP	TGGGAGCTTGATTCTCAGCA	CCTGGGCTTGACCTCTCTGTA	NM_002055
MAP-2	TTGGTGCCGAGTGAGAAGAA	GGTCTGGCAGTGGTTGGTTAA	NM_002374
NF-M	GTGAACCACGAGAAGGCTCA	AGGTAGTCTTTGCGCTCCAC	NM_005382
KCNH1	TTGGAGATGTGTTCTGGAAGGAA	AGGGCATCCCGCTTGATC	NM_172362.2
KCNH5	GACGAAATTTGCCCGATTGA	TGAATGTTTATGGACCACCTCTGT	AF_418206.1
Nanog	GTCCCAAAGGCAAACAACCC	GCTGGGTGGAAGAGAACACA	NM_024865
Oct-4	GCCCGAAAGAGAAAGCGAAC	AACCACACTCGGACCACATC	NM_002701
ALP	GCACCATGAAGGAAAAGCCA	TGTGAAGACGTGGGAATGGT	NM_000478
Adiponectin	ACATGCCCATTCGCTTTACC	AGAGGCTGACCTTCACATCC	NM_001177800
FABP4	GGCATGGCCAAACCTAACAT	CCTGGCCCAGTATGAAGGAA	NM_001442
MMP13	TTCCCAGTGGTGGTGATGAA	CAGGATTCCCGCGAGATTTG	NM_002427
β-actin	ATCCGCAAAGACCTGTACGC	TCTTCATTGTGCTGGGTGCC	NM_001101

Acc. No. indicates gene access number.

II-3. (4,5-Dimethylthiazol-2-yl-) 2,5-diphenyltetrazolium bromide (MTT) assay

The cell viabilities of rolipram-treated MSCs were evaluated by MTT assay (Sigma-Aldrich, St. Louis, MO, USA) performed according to the manufacturer's instructions. Briefly, 2.5 × 10^3 hBM-MSCs were seeded onto 96-well plates. The next day, the cells were incubated with 0–25 μM of rolipram for 12 h and subjected to MTT assay.

II-4. Neuronal differentiation

hBM-MSCs were incubated with/without 1 μM rolipram for 12 h. The cells were then exposed to pre-induction media (DMEM containing 10% (*v/v*) FBS, 10 ng/mL basic fibroblast growth factor, and 500 μM β-mercaptoethanol) for 24 h. The media was replaced with induction media containing 100 μM butylated hydroxyanisole and 2% (*v/v*) dimethyl sulfoxide in FBS-free media for 6 h, according to previously described procedures [2,3,4]. Control MSCs were incubated with FBS-containing media for 24 h. The media were replaced with FBS-free media and the cells were further incubated for 6 h. Images were captured with a microscope (Eclipse TS100; Nikon, Tokyo, Japan) and a digital camera (i-Solution IMTcam3; JENOPTIK, Jena, Germany). Cells were considered as differentiated neuronal cells when each cell body had more than 2 dendrites longer than 60 μm. Neurite lengths

were measured using the ImageJ program (NIH, Bethesda, MD, USA).

II-5. Immunocytochemical staining

hBM-MSCs were grown on poly-L-lysine-coated coverslips (Fisher Scientific, Hampton, NH, USA) and induced to differentiate into neuron-like cells. Cells were then subjected to immunocytochemical staining with antibodies against Nestin, NF-M or Tuj-1 (Santa Cruz biotechnology, Dallas, TX, USA) diluted 1:200 in blocking buffer overnight at 4 °C, and subsequently, with Alexa Fluor® 488-conjugated donkey anti-goat IgG or Alexa Fluor® 555-conjugated donkey anti-mouse IgG secondary antibodies (Molecular Probes Inc., Carlsbad, CA, USA) diluted 1:500 in Hoechst 33342 (Molecular Probes Inc.) for 1 h at room temperature. The cells were visualized by fluorescence microscopy with a Nikon Eclipse 80Ti microscope (Nikon, Tokyo, Japan). Cell images were taken with a DS-RI1 digital camera (Nikon).

II-6. Immunoblot analysis

Cells were extracted with 400 μL radioimmunoprecipitation assay buffer containing protease and phosphatase inhibitors (Santa Cruz Biotechnology) for 30 min at 4 °C and then centrifuged at 16,000 × *g* for 20 min. Total protein was then subjected to immunoblotting with antibodies against NF-M (1:500), Nestin (1:500), Tuj-1 (1:1000), Musashi (1:500), GFAP (1:500),

Sox-2 (1:500) or β-actin (1:5,000), and subsequently, the appropriate horseradish peroxidase-conjugated secondary antibodies (1:10,000; Jackson Immuno Research Laboratories, West Grove, PA, USA). Band densities were quantified with the ImageJ program (NIH).

II-7. Statistical analysis

The data are represented as the mean ± standard deviation (SD) of 3 or more independent experiments. Statistical comparisons between groups were made using independent samples *t*-tests. P-values < 0.05 were considered statistically significant.

III. Results

III-1. Neuroprogenitor gene markers are induced by rolipram in hBM-MSCs

To evaluate the dose effects of rolipram, hBM-MSCs were incubated with 0-25 μM of rolipram for 12 h. The expression of the neuroprogenitor markers *Nestin* and *CD133* was assessed by qPCR. As shown in Figure 1A, the expression of these genes was increased by rolipram treatment in a dose-dependent manner at doses ≤ 1 μM and was decreased at higher doses. (Fig. 1A; *t*-test, $*p < 0.05$, $**p < 0.005$, mean ± SD, n=4). To determine the optimal time of rolipram treatment in hBM-MSCs, MSCs were incubated with 1 μM rolipram for several different periods of time (0–24 h). Expression of the tested genes peaked after incubation for 12 h (Fig. 1B; *t*-test, $*p < 0.05$, $**p < 0.005$, mean ± SD, n=3). Cellular toxicity was not observed at doses of ≤ 5 μM rolipram for 12 h (Fig. 1C; *t*-test, $*p < 0.05$, mean ± SD, n=3). From these data, I determined that treatment with 1 μM rolipram for 12 h was the optimal condition. I have shown that rolipram stimulates the expression of neuroprogenitor genes under the optimized treatment condition (Fig. 1A-C). To further evaluate the role of rolipram in regulating cell fate, additional neuroprogenitor genes were measured by qPCR. The expression of the neuroprogenitor genes *Nestin*, *Musashi*, *CD133* and *GFAP* was significantly increased in rolipram-treated hBM-MSCs (Roli-MSCs) compared with that of the non-treated hBM-MSCs (Fig. 1D;

t-test, $*p < 0.05$, $**p < 0.005$, mean ± SD, n=3). Similarly, the increased protein levels of Nestin, Musashi, GFAP and Sox-2 were confirmed by immunoblot analysis (Fig. 1E).

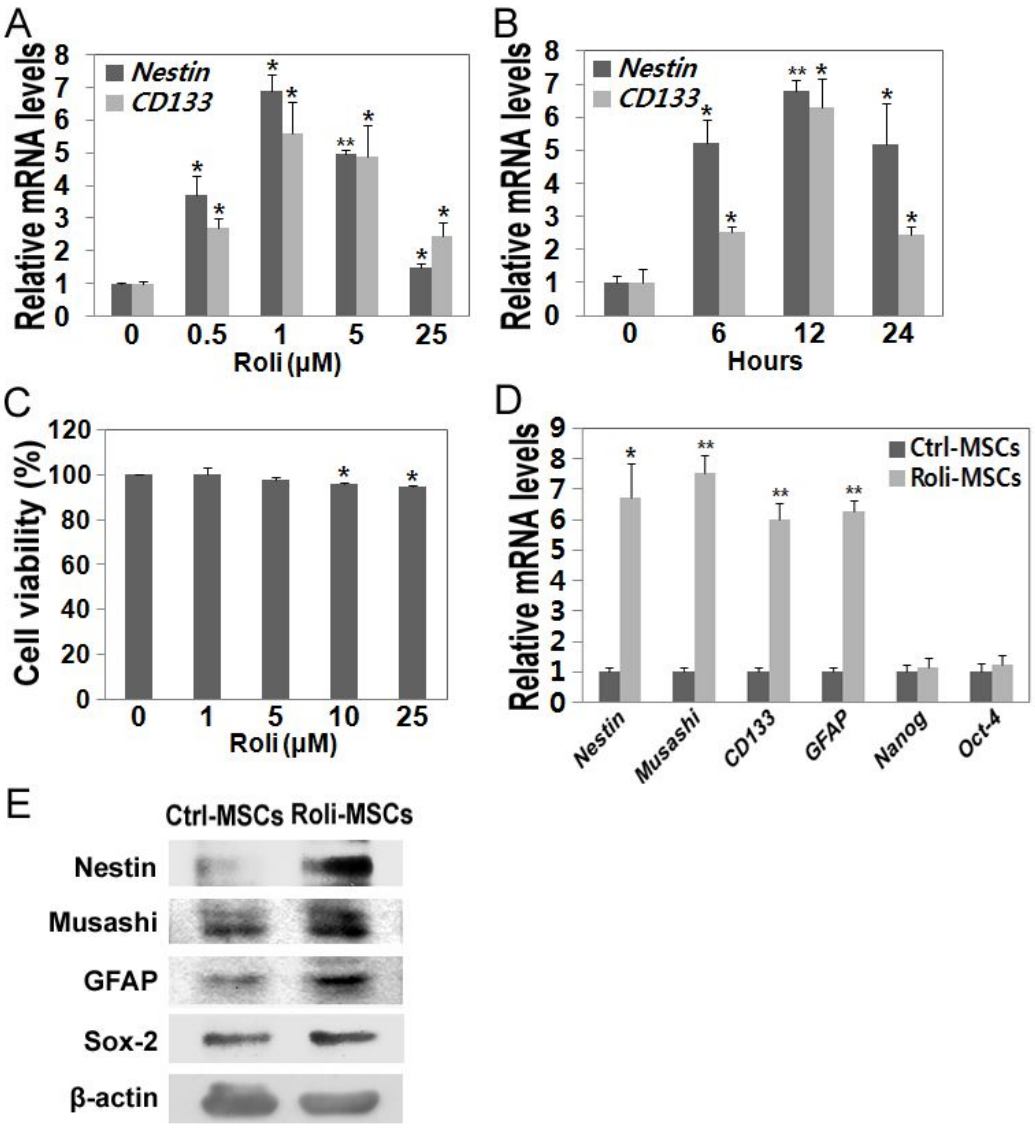

Figure 1. Rolipram induces the expression of neuroprogenitor markers in hBM-MSCs.

(A) hBM-MSCs were treated with 0–25 μM of rolipram for 12 h. The expression of the neuroprogenitor genes *Nestin* and *CD133* was identified by qPCR. (B) 1 μM rolipram was applied for various incubation times (0–24 h), then the expression levels of *Nestin* and *CD133* were measured by qPCR. (C) Cytotoxicity was estimated after treating MSCs with a dose range of 0–25 μM rolipram for 12 h. (D) MSCs were treated with 1 μM rolipram for 12 h and the expression of neuroprogenitor marker genes was measured by qPCR. Expression levels of the neuroprogenitor markers *Nestin*, *Musashi*, *CD133* and *GFAP* were significantly increased in rolipram-treated hBM-MSCs (Roli-MSCs) compared with those of non-treated hBM-MSCs (Ctrl-MSCs). (E) The protein expression of neuroprogenitor markers was confirmed by immunoblot analysis using antibodies specific to Nestin, Musashi, GFAP, Sox-2 and β-actin.

III-2. Rolipram-pretreated hBM-MSCs have a neuronal appearance in neuronal induction media

After I had identified the induction of the expression of neuronal progenitor genes by rolipram treatment in MSCs, I hypothesized that Roli-MSCs could be more effectively differentiated into neuronal cells than control MSCs (Ctrl-MSCs) could be. To evaluate this hypothesis, both Ctrl-MSCs and Roli-MSCs were differentiated with neuronal induction media [16,29]. Both neuronally differentiated MSCs (Fig. 2A; dMSCs and Roli-dMSCs) exhibited neuronal morphology, while undifferentiated BM-MSCs (Ctrl-MSCs) and Roli-MSCs showed a flattened and spindle-shaped appearance similar to that of primary hBM-MSCs (Fig. 2A; Ctrl-MSCs and Roli-MSCs). Roli-dMSCs showed a significantly higher estimated rate of differentiation into neuron-like cells than did dMSCs (Fig. 2B and Table 2; *t*-test, $*p < 0.05$, mean ± SD, n=4). The average neurite length of dMSCs was also significantly greater in Roli-dMSCs than dMSCs (Fig. 2C, 2D and Table 3; *t*-test, $*p < 0.05$, $**p < 0.005$, mean ± SD, n=4), and a significant difference in the number of neurites was observed for dMSCs vs. Roli-dMSCs (Fig. 2D).

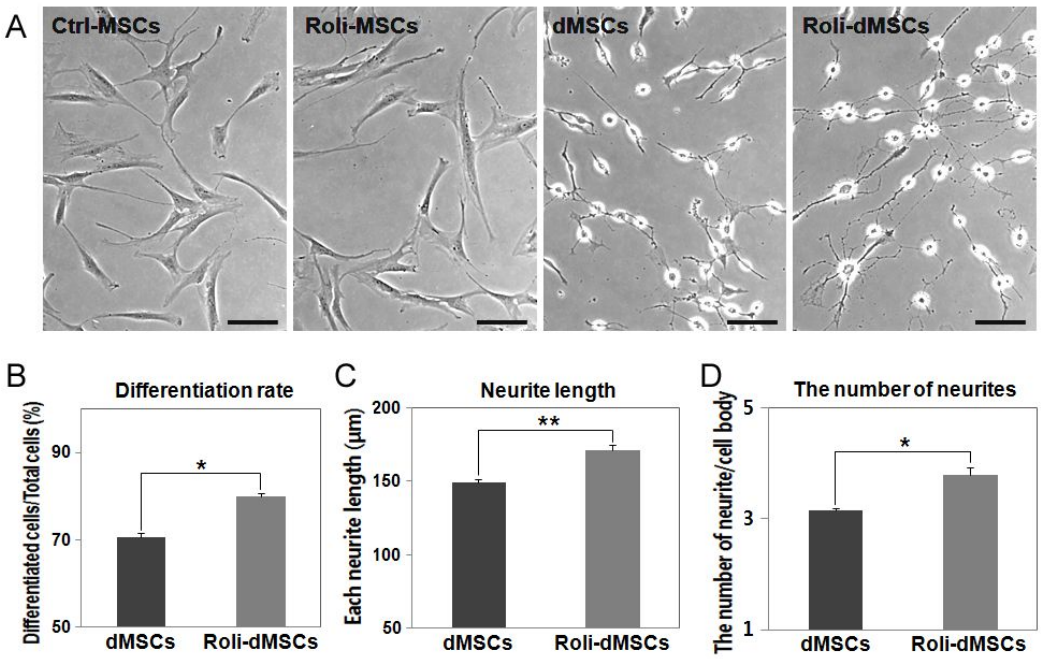

Figure 2. Neuron-like morphological changes in Roli-MSCs followed by neuronal induction.

(A) Both Ctrl-MSCs and Roli-MSCs were differentiated into neuronal cells following exposure to neuronal induction media. Differentiated MSCs (dMSCs) and rolipram-treated dMSCs (Roli-dMSCs) are shown. The scale bar indicates 100 μm. (B) Total cells and neuronal-shaped cells were counted to estimate the neuronal differentiation rate. Roli-dMSCs underwent differentiation at a significantly higher rate compared with that of dMSCs. (C) The mean neurite length was significantly longer in Roli-dMSCs than dMSCs. (D) The number of neurites was significantly increased in differentiated cells compared with that of undifferentiated cells.

Table 2. The neuronal-like cells were counted to estimate the neuronal differentiation rate

Experiments (n=4)	dMSCs (Differentiated cells/total cells)	Roli-dMSCs (Differentiated cells/total cells)
1st	264 / 364	282 / 361
2nd	765 / 1103	926 / 1149
3rd	597 / 857	639 / 791
4th	435 / 619	525 / 638
Sum	2061 / 2943 (75.1%)	2372 / 2939 (83.8%)

Table 3. The number of neurites from each differentiated cells were counted and neurite lengths were measured.

dMSCs			
Experiments (n=4)	Total cells	The No. of Neurite (Ave/each cell)	Neurite length (Ave/each neurite, ㎛)
1st	115	3.08	150.44
2nd	80	3.23	147.99
3rd	152	3.22	154.51
4th	123	3.15	153.80
Ave.	117.5	3.17	151.685

Roli-dMSCs			
Experiments (n=4)	Total cells	The No. of Neurite (Ave/each cell)	Neurite length (Ave/each neurite, ㎛)
1st	85	3.57	167.56
2nd	78	3.41	175.60
3rd	153	3.71	178.26
4th	135	4.07	179.12
Ave.	112.75	3.69	175.135

III-3. Increased expression of diverse neuronal markers in dMSCs treated with rolipram

Since Roli-dMSCs have a neuronal appearance, the expression of various neuronal-specific marker genes was evaluated by qPCR (Fig. 3A). The expression levels of all the neuronal marker genes tested in this study were significantly increased in both Roli-dMSCs and dMSCs compared with those of the undifferentiated MSCs (Ctrl-MSCs) (Fig. 3A; *t*-test, $*p < 0.05$, $**p < 0.005$, mean ± SD, n=5). The expression of neuronal-specific marker genes (*CD133*, *NF-M, MAP-2* and *KCNH5)* was significantly increased in Roli-dMSCs compared with that of dMSCs (Fig. 3A; *t*-test, $*p < 0.05$, $**p < 0.005$, mean ± SD, n=5). I also examined the expression of other lineage specific markers in dMSCs and Roli-dMSCs, and I identified decreased expression levels of osteogenic (*ALP*), adipogenic (*Adiponectin* and *FABP4*) and chondrogenic (*MMP13*) specific genes in dMSCs and Roli-dMSCs compared with those of the Ctrl-MSCs (Fig. 3B; *t*-test, $**p < 0.005$, mean ± SD, n=4).

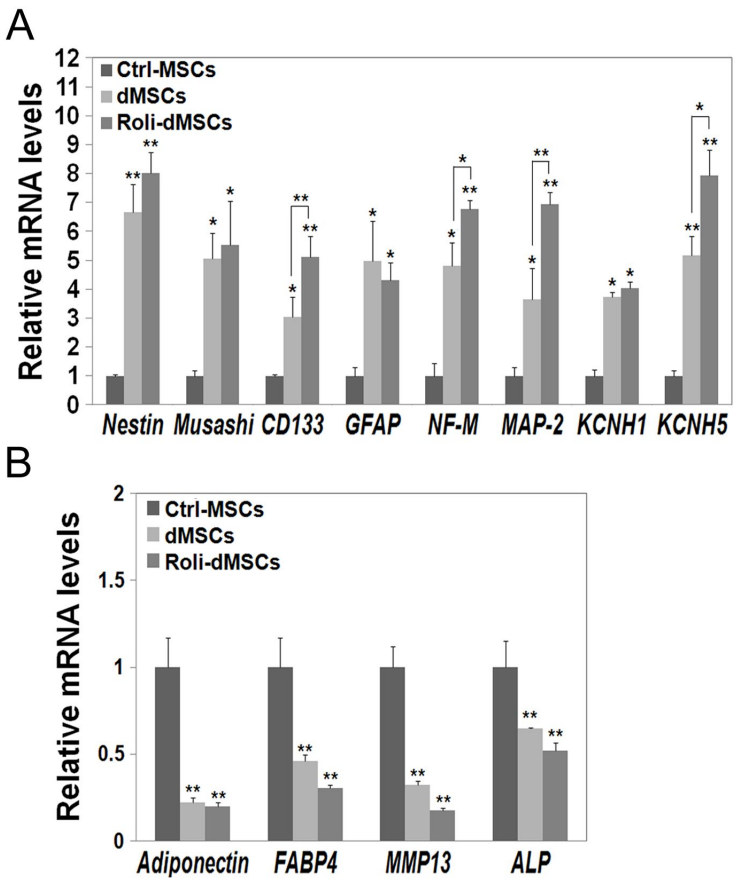

Figure 3. Increased expression of diverse neuronal markers in differentiated, rolipram-treated MSCs.

(A) The expression of several neuronal specific genes was measured in MSCs (Ctrl-MSCs), differentiated MSCs (dMSCs), and rolipram-treated dMSCs (Roli-dMSCs) by qPCR. The expression levels of all genes tested in this experiment were significantly increased in differentiated MSCs compared with those of undifferentiated MSCs. The expression levels of *CD133, NF-M, MAP-2* and *KCNH5* were significantly increased in Roli-dMSCs compared with those of dMSCs. (B) The expression levels of osteogenic, adipogenic and chondrogenic specific genes were decreased in both dMSCs and Roli-dMSCs compared with those of Ctrl-MSCs.

III-4. Neuronal-specific proteins are up-regulated in rolipram pre-treated dMSCs.

To characterize whether the expression levels of markers of neuronal differentiation were changed at the protein level, I used an immunocyto-chemical staining assay. Ctrl-MSCs, dMSCs and Roli-dMSCs were fixed and stained with specific antibodies against the neuronal marker proteins Nestin, NF-M and Tuj-1. Neuronal-induced MSCs (dMSCs) and Roli-dMSCs exhibited positive cytoplasmic staining for Nestin, NF-M and Tuj-1, while the non-induced MSCs were negative for these markers (Ctrl-MSCs; Fig. 4A). Similar results were obtained by immunoblot analysis using antibodies specific to Nestin, Musashi, Sox-2, NF-M and Tuj-1 (Fig. 4B).

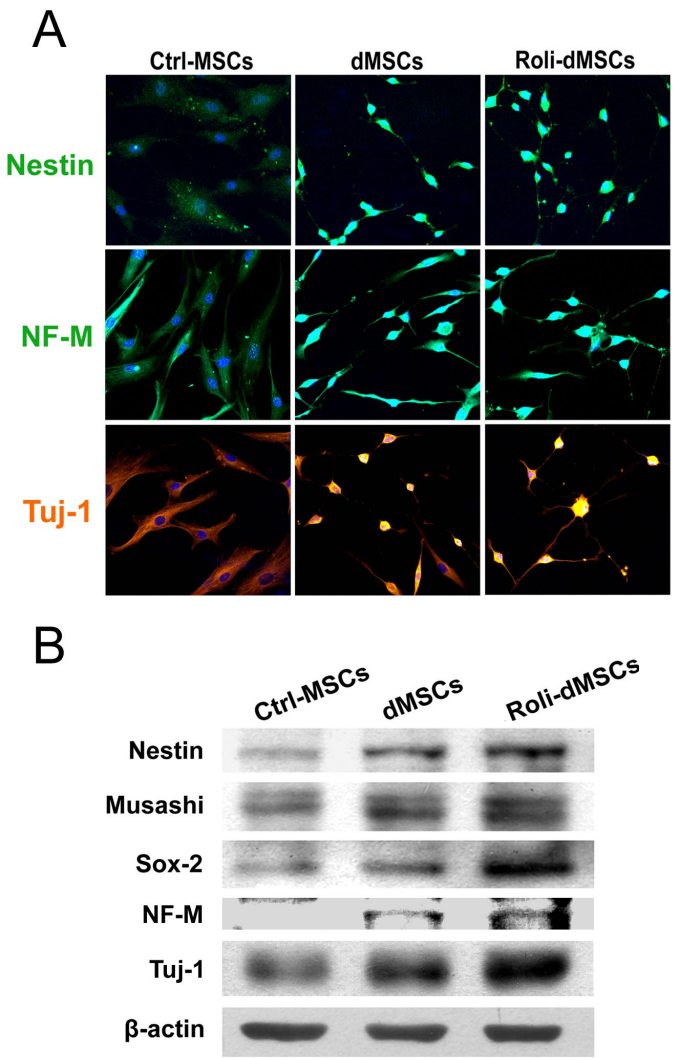

Figure 4. Up-regulation of neuronal-specific proteins in Roli-dMSCs.
(A) MSCs (Ctrl-MSCs) and differentiated MSCs (dMSCs, Roli-dMSCs) were fixed and stained with antibodies for the specific neuronal markers Nestin (upper panel), NF-M (middle panel) and Tuj-1 (lower panel), and visualized by fluorescent microscopy. (B) The MSCs were subjected to immunoblot analysis with antibodies for Nestin, Musashi, Sox-2, NF-M and Tuj-1. β-actin was used as an internal standard.

IV. Discussion

Increasing cAMP involves diverse cellular physiological processes including neuronal differentiation [38,49]. Failure of the cellular mechanisms that normally regulate intracellular cAMP homeostasis contributes to diverse neurological diseases [39-41]. Inhibition of the cAMP-hydrolyzing enzyme phosphodiesterase 4 (PDE4) improves these diseases [40,43-48], suggesting that PDE4 may be an important therapeutic target for these neurological diseases. In this study, I investigated whether the PDE4 selective inhibitor rolipram could facilitate neuronal differentiation in hBM-MSCs. Rolipram-treated MSCs showed an increased expression of neuronal progenitor genes under optimized treatment conditions (1 μM for 12 h; Fig. 1). When cultured with neuronal induction media [16,29], Roli-dMSCs showed significant increases in the expression of neuronal-specific markers and the rate of neuronal differentiation, compared with those of dMSCs (Fig. 2, 3 and 4).

Increasing the levels of intracellular cAMP has been shown to sustain neuronal architecture by stimulating axon elongation and neurite outgrowth [33,34]. When using rolipram as a PDE4 inhibitor in this study, both neurite lengths and the number of neurites were significantly increased in Roli-dMSCs. The expression levels of the dendritic specific gene *MAP-2* and the axonal marker Tuj-1 [50] were both elevated in Roli-dMSCs compared with those of dMSCs (Fig. 3 and 4). This suggests that Roli-MSCs had greater neurite outgrowth and a higher rate of differentiation into neuron-like cells

than did the Ctrl-MSCs in the presence of neuronal induction media.

I have shown that hBM-MSCs effectively differentiated into neuron-like cells following rolipram treatment. However, the signaling pathways directly involved in this process have not been confirmed. Rolipram treatment increases intracellular cAMP by inhibiting PDE4 enzyme activity. The elevated cAMP may activate protein kinase A (PKA) and cAMP-responsive element-binding protein (CREB), subsequently leading to the increased expression of several genes, potentially including genes associated with neuronal induction [44]. Previous studies have shown that PDE4 inhibition improves symptoms in neurodegenerative disease models [44-47] and enhances the differentiation capacity of stem cells [38,49,51], which supports our results.

hBM-MSCs, which have the capacity to differentiate into neurons [16,29,52], have been used for cell therapy in neurodegenerative diseases [3]. However, only a few cells were successfully differentiated into neurons when this approach was attempted in an in vivo animal study [8], suggesting that the differentiation potency of donor stem cells should be improved prior to cell therapy. In this study, I have shown that Roli-MSCs endogenously induced the expression of neuroprogenitor marker proteins that synergistically facilitated neuronal differentiation in the presence of neuronal induction media. Thus, Roli-MSCs may enhance neuronal differentiation and thereby improve the efficacy of stem cell therapy for neurodegenerative diseases.

CONCLUSION

I have demonstrated that SIRT1 activators (resveratrol and rolipram) improved neuronal differentiation in hBM-MSCs and also identified that resveratrol and rolipram promoted neuronal differentiation by the induction of neuroprogenitors in hBM-MSCs. Thus, resveratrol- or rolipram-pretreated MSCs may provide advances in stem cell therapy for neurodegenerative disorders.

REFERENCES

[1] J.A. Baur, K.J. Pearson, N.L. Price, H.A. Jamieson, C. Lerin, A. Kalra, V.V. Prabhu,J.S. Allard, G. Lopez-Lluch, K. Lewis, P.J. Pistell, S. Poosala, K.G. Becker, O. Boss, D.Gwinn, M. Wang, S. Ramaswamy, K.W. Fishbein, R.G. Spencer, E.G. Lakatta, D. LeCouteur, R.J. Shaw, P. Navas, P. Puigserver, D.K. Ingram, R. de Cabo, D.A. Sinclair, Resveratrol improves health and survival of mice on a high-calorie diet, Nature444 (2006) 337–342.

[2] A.I. Caplan, Adult mesenchymal stem cells for tissue engineering versus regenerative medicine, J. Cell. Physiol. 213 (2007) 341–347.

[3] E. Dantuma, S. Merchant, K. Sugaya, Stem cells for the treatment of neurodegenerative diseases, Stem Cell Res. Ther. 1 (2010) 37.

[4] G. Donmez, The Effects of SIRT1 on Alzheimer's disease models, Int. J. Alzheimers Dis. 2012 (2012) 509529.

[5] G. Donmez, The neurobiology of sirtuins and their role in neurodegeneration, Trends Pharmacol. Sci. 33 (2012) 494–501.

[6] G. Donmez, A. Arun, C.Y. Chung, P.J. McLean, S. Lindquist, L. Guarente, SIRT1 pro-tects against alpha-synuclein aggregation by activating molecular chaperones, J. Neurosci. 32 (2012) 124–132.

[7] G. Donmez, D. Wang, D.E. Cohen, L. Guarente, SIRT1 suppresses beta-amyloid production by activating the alpha-secretase gene ADAM10, Cell 142 (2010)320–332.

[8] W. Fan, K. Cheng, X. Qin, K.H. Narsinh, S. Wang, S. Hu, Y. Wang, Y. Chen, J.C. Wu,L. Xiong, F. Cao, mTORC1 and mTORC2 play different roles in the functional survival of transplanted adipose-derived stromal cells in hind limb ischemic mice via regulating inflammation in vivo, Stem Cells 31 (2013) 203–214.

[9] W. Guo, L. Qian, J. Zhang, W. Zhang, A. Morrison, P. Hayes, S. Wilson, T. Chen,J. Zhao, Sirt1 over expression in neurons promotes neurite outgrowth and cell survival through inhibition of the mTOR signaling, J. Neurosci. Res. 89 (2011)1723–1736.

[10] S. Han, J.R. Choi, K. Soon Shin, S.J. Kang, Resveratrol up regulated

heat shock proteins and extended the survival of G93A-SOD1 mice, Brain Res. 1483 (2012)112–117.

[11] A.Z. Herskovits, L. Guarente, SIRT1 in neurodevelopment and brain senescence, Neuron 81 (2014) 471–483.

[12] K.R. Holloway, T.N. Calhoun, M. Saxena, C.F. Metoyer, E.F. Kandler, C.A. Rivera,K. Pruitt, SIRT1 regulates dishevelled proteins and promotes transient and constitutive Wnt signaling, Proc. Natl. Acad. Sci. U.S.A. 107 (2010) 9216–9221.

[13] K.T. Howitz, K.J. Bitterman, H.Y. Cohen, D.W. Lamming, S. Lavu, J.G. Wood, R.E. Zipkin, P. Chung, A. Kisielewski, L.L. Zhang, B. Scherer, D.A. Sinclair, Small molecule activators of sirtuins extend Saccharo-myces cerevisiae lifespan, Nature425 (2003) 191–196.

[14] S.C. Hsu, S.M. Huang, A. Chen, C.Y. Sun, S.H. Lin, J.S. Chen, S.T. Liu, Y.J. Hsu, Resveratrol increases anti-aging Klotho gene expression via the activating transcription factor 3/c-Jun complex-mediated signaling pathway, Int. J. Biochem. Cell Biol. 53 (2014) 361–371.

[15] H. Jeong, D.E. Cohen, L. Cui, A. Supinski, J.N. Savas, J.R. Mazzulli, J.R. Yates 3rd, L. Bordone, L. Guarente, D. Krainc, Sirt1 mediates neuroprotection from mutant huntington by activation of the TORC1 and CREB transcriptional pathway, Nat. Med. 18 (2012) 159–165.

[16] S.G. Jeong, T. Ohn, S.H. Kim, G.W. Cho, Valproic acid promotes neuronal differentiation by induction of neuroprogenitors in human bone-marrow mesenchymal stromal cells, Neurosci. Lett. 554 (2013) 22–27.

[17] X.H. Li, C. Chen, Y. Tu, H.T. Sun, M.L. Zhao, S.X. Cheng, Y. Qu, S. Zhang, Sirt1promotes axonogenesis by deacetylation of Akt and inactivation of GSK3, Mol. Neurobiol. 48 (2013) 490–499.

[18] J.C. Milne, P.D. Lambert, S. Schenk, D.P. Carney, J.J. Smith, D.J. Gagne, L. Jin, O.Boss, R.B. Perni, C.B. Vu, J.E. Bemis, R. Xie, J.S. Disch, P.Y. Ng, J.J. Nunes, A.V. Lynch,H. Yang, H. Galonek, K. Israelian, W. Choy, A. Iffland, S. Lavu, O. Medvedik, D. A. Sinclair, J.M. Olefsky, M.R. Jirousek, P.J. Elliott, C.H. Westphal, Small molecule activators of SIRT1 as therapeutics for the treatment of type 2 diabetes, Nature450 (2007) 712–716.

[19] M. Pallas, G. Casadesus, M.A. Smith, A. Coto-Montes, C. Pelegri, J.

Vilaplana,A. Camins, Resveratrol and neurodegenerative diseases: activation of SIRT1 asthe potential pathway towards neuroprotection, Curr. Neurovasc. Res. 6 (2009)70–81.

[20] S.J. Park, F. Ahmad, A. Philp, K. Baar, T. Williams, H. Luo, H. Ke, H. Rehmann,R. Taussig, A.L. Brown, M.K. Kim, M.A. Beaven, A.B. Burgin, V. Manganiello, J.H.Chung, Resveratrol ameliorates aging-related metabolic phenotypes by inhibiting cAMP phosphodiesterases, Cell 148 (2012) 421–433.

[21] M.F. Pittenger, A.M. Mackay, S.C. Beck, R.K. Jaiswal, R. Douglas, J.D. Mosca, M. A. Moorman, D.W. Simonetti, S. Craig, D.R. Marshak, Multilineage potential of adult human mesenchymal stem cells, Science 284 (1999) 143–147.

[22] N.L. Price, A.P. Gomes, A.J. Ling, F.V. Duarte, A. Martin-Montalvo, B.J. North, B. Agarwal, L. Ye, G. Ramadori, J.S. Teodoro, B.P. Hubbard, A.T. Varela, J.G. Davis,B. Varamini, A. Hafner, R. Moaddel, A.P. Rolo, R. Coppari, C.M. Palmeira, R. deCabo, J.A. Baur, D.A. Sinclair, SIRT1 is required for AMPK activation and the beneficial effects of resveratrol on mitochondrial function, Cell Metab. 15 (2012)675–690.

[23] V.R. Ramprasath, P.J. Jones, Anti-atherogenic effects of resveratrol, Eur. J. Clin. Nutr. 64 (2010) 660–668.

[24] C.K. Singh, A. Kumar, H.A. Lavoie, D.J. Dipette, U.S. Singh, Diabetic complications in pregnancy: is resveratrol a solution? Exp. Biol. Med. (Maywood) 238 (2013)482–490.

[25] J.M. Solomon, R. Pasupuleti, L. Xu, T. McDonagh, R. Curtis, P.S. DiStefano, L. J. Huber, Inhibition of SIRT1 catalytic activity increases p53 acetylation but does not alter cell survival following DNA damage, Mol. Cell Biol. 26 (2006)28–38.

[26] T. Sugino, M. Maruyama, M. Tanno, A. Kuno, K. Houkin, Y. Horio, Protein deacetylase SIRT1 in the cytoplasm promotes nerve growth factor-induced neurite outgrowth in PC12 cells, FEBS Lett. 584 (2010) 2821–2826.

[27] A.L. Widlund, J.A. Baur, O. Vang, mTOR: more targets of resveratrol? Expert Rev.Mol. Med. 15 (2013) e10.

[28] J.G. Wood, B. Rogina, S. Lavu, K. Howitz, S.L. Helfand, M. Tatar, D. Sinclair, Sirtuin activators mimic caloric restriction and delay ageing in

metazoans, Nature 430(2004) 686–689.

[29] I.S. Joe, S.G. Jeong, G.W. Cho, Resveratrol-induced SIRT1 activation promotes neuronal differentiation of human bone marrow mesenchymal stem cells, Neurosci Lett 584 (2015) 97-102.

[30] A. Uccelli, M. Milanese, M.C. Principato, S. Morando, T. Bonifacino, L. Vergani, D. Giunti, A. Voci, E. Carminati, F. Giribaldi, C. Caponnetto, G. Bonanno, Intravenous mesenchymal stem cells improve survival and motor function in experimental amyotrophic lateral sclerosis, Mol Med 18 (2012) 794-804.

[31] F. Blandini, L. Cova, M.T. Armentero, E. Zennaro, G. Levandis, P. Bossolasco, C. Calzarossa, M. Mellone, B. Giuseppe, G.L. Deliliers, E. Polli, G. Nappi, V. Silani, Transplantation of undifferentiated human mesenchymal stem cells protects against 6-hydroxydopamine neurotoxicity in the rat, Cell Transplant 19 (2010) 203-217.

[32] J. Chen, Y. Li, M. Katakowski, X. Chen, L. Wang, D. Lu, M. Lu, S.C. Gautam, M. Chopp, Intravenous bone marrow stromal cell therapy reduces apoptosis and promotes endogenous cell proliferation after stroke in female rat, J Neurosci Res 73 (2003) 778-786.

[33] A. Blesch, P. Lu, S. Tsukada, L.T. Alto, K. Roet, G. Coppola, D. Geschwind, M.H. Tuszynski, Conditioning lesions before or after spinal cord injury recruit broad genetic mechanisms that sustain axonal regeneration: superiority to camp-mediated effects, Exp Neurol 235 (2012) 162-173.

[34] S. Neumann, C.J. Woolf, Regeneration of dorsal column fibers into and beyond the lesion site following adult spinal cord injury, Neuron 23 (1999) 83-91.

[35] S. Neumann, F. Bradke, M. Tessier-Lavigne, A.I. Basbaum, Regeneration of sensory axons within the injured spinal cord induced by intraganglionic cAMP elevation, Neuron 34 (2002) 885-893.

[36] J. Qiu, D. Cai, H. Dai, M. McAtee, P.N. Hoffman, B.S. Bregman, M.T. Filbin, Spinal axon regeneration induced by elevation of cyclic AMP, Neuron 34 (2002) 895-903.

[37] D. Cai, J. Qiu, Z. Cao, M. McAtee, B.S. Bregman, M.T. Filbin, Neuronal cyclic AMP controls the developmental loss in ability of axons to regenerate, J Neurosci 21 (2001) 4731-4739.

[38] L. Zhang, L.C. Seitz, A.M. Abramczyk, L. Liu, C. Chan, cAMP initiates early phase neuron-like morphology changes and late phase neural differentiation in mesenchymal stem cells, Cell Mol Life Sci 68 (2011) 863-876.

[39] J.M. O'Donnell, H.T. Zhang, Antidepressant effects of inhibitors of cAMP phosphodiesterase (PDE4), Trends Pharmacol Sci 25 (2004) 158-163.

[40] A. Garcia-Osta, M. Cuadrado-Tejedor, C. Garcia-Barroso, J. Oyarzabal, R. Franco, Phosphodiesterases as therapeutic targets for Alzheimer's disease, ACS Chem Neurosci 3 (2012) 832-844.

[41] J.A. Siuciak, D.S. Chapin, S.A. McCarthy, A.N. Martin, Antipsychotic profile of rolipram: efficacy in rats and reduced sensitivity in mice deficient in the phosphodiesterase-4B (PDE4B) enzyme, Psychopharmacology (Berl) 192 (2007) 415-424.

[42] W. Krause, G. Kuhne, N. Sauerbrey, Pharmacokinetics of (+)-rolipram and (-)-rolipram in healthy volunteers, Eur J Clin Pharmacol 38 (1990) 71-75.

[43] N. Kumar, A.M. Goldminz, N. Kim, A.B. Gottlieb, Phosphodiesterase 4-targeted treatments for autoimmune diseases, BMC Med 11 (2013) 96.

[44] B. Gong, O.V. Vitolo, F. Trinchese, S. Liu, M. Shelanski, O. Arancio, Persistent improvement in synaptic and cognitive functions in an Alzheimer mouse model after rolipram treatment, J Clin Invest 114 (2004) 1624-1634. [22] C. Normann, M. Berger, Neuroenhancement: status quo and perspectives, Eur Arch Psychiatry Clin Neurosci 258 Suppl 5 (2008) 110-114.

[45] Z. DeMarch, C. Giampa, S. Patassini, A. Martorana, G. Bernardi, F.R. Fusco, Beneficial effects of rolipram in a quinolinic acid model of striatal excitotoxicity, Neurobiol Dis 25 (2007) 266-273.

[46] C.M. Atkins, A.A. Oliva, Jr., O.F. Alonso, D.D. Pearse, H.M. Bramlett, W.D. Dietrich, Modulation of the cAMP signaling pathway after traumatic brain injury, Exp Neurol 208 (2007) 145-158.

[47] S.S. Hannila, M.T. Filbin, The role of cyclic AMP signaling in promoting axonal regeneration after spinal cord injury, Exp Neurol 209 (2008) 321-332.

[48] Z. Huang, J.A. Mancini, Phosphodiesterase 4 inhibitors for the treatment of asthma and COPD, Curr Med Chem 13 (2006) 3253-3262.

[49] W. Deng, M. Obrocka, I. Fischer, D.J. Prockop, In vitro differentiation of human marrow stromal cells into early progenitors of neural cells by conditions that increase intracellular cyclic AMP, Biochem Biophys Res Commun 282 (2001) 148-152.

[50] P.F. Moskowitz, M.M. Oblinger, Sensory neurons selectively upregulate synthesis and transport of the beta III-tubulin protein during axonal regeneration, J Neurosci 15 (1995) 1545-1555.

[51] S.S. Kim, J.M. Choi, J.W. Kim, D.S. Ham, S.H. Ghil, M.K. Kim, Y. Kim-Kwon, S.Y. Hong, S.C. Ahn, S.U. Kim, Y.D. Lee, H. Suh-Kim, cAMP induces neuronal differentiation of mesenchymal stem cells via activation of extracellular signal-regulated kinase/MAPK, Neuroreport 16 (2005) 1357-1361.

[52] J.N. Francischi, C.M. Yokoro, S. Poole, W.L. Tafuri, F.Q. Cunha, M.M. Teixeira, Anti-inflammatory and analgesic effects of the phosphodiesterase 4 inhibitor rolipram in a rat model of arthritis, Eur J Pharmacol 399 (2000) 243-249.

[53] C. Normann, M. Berger, Neuroenhancement: status quo and perspectives, Eur Arch Psychiatry Clin Neurosci 258 Suppl 5 (2008) 110-114.